Social Cognitive and Affective Neuroscience, 2021, 232–245

doi:10.1093/scan/nsaa130
Advance Access Publication Date: 12 October 2020
Original Manuscript

Interpersonal Synchrony Special Issue

Windowed multiscale synchrony: modeling time-varying and scale-localized interpersonal coordination dynamics

Aaron D. Likens[1] and Travis J. Wiltshire[2]

[1]Department of Biomechanics, University of Nebraska at Omaha, 6001 Dodge Street Omaha, NE 68182 and [2]Department of Cognitive Science & Artificial Intelligence, Tilburg University, (Room D104) Warandelaan 2, 5037 AB, Tilburg, The Netherlands

Correspondence should be addressed to Aaron D. Likens, Department of Biomechanics University of Nebraska at Omaha 6001 Dodge Street Omaha, NE 68182. E-mail:alikens@unomaha.edu

Abstract

Social interactions are pervasive in human life with varying forms of interpersonal coordination emerging and spanning different modalities (e.g. behaviors, speech/language, and neurophysiology). However, during social interactions, as in any dynamical system, patterns of coordination form and dissipate at different scales. Historically, researchers have used aggregate measures to capture coordination over time. While those measures (e.g. mean relative phase, cross-correlation, coherence) have provided a wealth of information about coordination in social settings, some evidence suggests that multiscale coordination may change over the time course of a typical empirical observation. To address this gap, we demonstrate an underutilized method, windowed multiscale synchrony, that moves beyond quantifying aggregate measures of coordination by focusing on how the relative strength of coordination changes over time and the scales that comprise social interaction. This method involves using a wavelet transform to decompose time series into component frequencies (i.e. scales), preserving temporal information and then quantifying phase synchronization at each of these scales. We apply this method to both simulated and empirical interpersonal physiological and neuromechanical data. We anticipate that demonstrating this method will stimulate new insights on the mechanisms and functions of synchrony in interpersonal contexts using neurophysiological and behavioral measures.

Key words: coordination; synchrony; multiscale; neurophysiology; dynamics

Introduction

Social interactions are pervasive in human life with varying forms of interpersonal coordination emerging and spanning different modalities (e.g. behaviors, speech/language, and neurophysiology). For example, couples, strangers, team members, and patient–therapist dyads tend to synchronize their heart rates and skin conductance during interactions (see Palumbo *et al.*, 2017 for review) and this occurs in multiple behavioral modalities too (e.g. Louwerse *et al.*, 2012). Increasingly, researchers have linked various forms of interpersonal

Received: 18 January 2020; **Revised:** 30 June 2020; **Accepted:** 18 September 2020

coordination to important constructs and outcomes in several areas including team work (Chanel *et al.*, 2013; Gorman, 2014; Likens *et al.*, 2014; Gorman *et al.*, 2016; Guastello and Peressini, 2017; Wiltshire *et al.*, 2018, 2019), relationship science (Butler, 2011; Randall *et al.*, 2013; Gottman, 2014; Perry *et al.*, 2017), conversational dynamics (Abney *et al.*, 2015; Fusaroli and Tylén, 2016), and clinical psychology (Ramseyer and Tschacher, 2011, 2014, 2016; Crowell *et al.*, 2017; Wiltshire *et al.*, 2020).

Importantly, during social interactions, as in any dynamical system, patterns of coordination form and dissipate at different spatiotemporal scales (Schmidt *et al.*, 1998; Dale *et al.*, 2013; Dumas *et al.*, 2014; Gorman *et al.*, 2019; Zhang *et al.*, 2019). In fact, recent theorizing emphasizes that moving in and out of synch with others is critical to adaptive human behavior (Mayo and Gordon, 2020) and that coordination in biological systems is fundamentally a multiscale phenomenon (Zhang *et al.*, 2019, 2020). Historically, researchers have used aggregate measures to capture coordination over time (see Delaherche *et al.*, 2012 for review). While those measures (e.g. mean relative phase, cross-correlation, coherence) have provided a wealth of information about coordination in social settings, because coordination is multiscale, it can occur differently at multiple spatial and/or temporal scales and also changes over the time course of a typical experiment (Tognoli *et al.*, 2007; Likens *et al.*, 2014; Fujiwara *et al.*, 2019; Wiltshire *et al.*, 2019).

With regard to interpersonal coordination at different scales, a recent set of studies found that rhythmic oscillations in human movements under 0.025 Hz and between 0.5 and 1.5 Hz were associated with increases in rapport between individuals (Fujiwara *et al.*, 2019). Similarly, in another study, movement coordination corresponding to temporal scales of 0.25 s and 1.0 s scales were found not only to relate to collaborative problem-solving performance, but the change in this coordination over the duration of the interaction was also indicative of task performance (Wiltshire *et al.*, 2019). In addition to movements, extant research suggests that neurophysiological signals also have varyingly important frequency components such as those that contribute to heart rate variability (Shaffer and Ginsberg, 2017) and brainwaves measured with electroencephalogram (EEG) (Keller *et al.*, 2014) and, for example, hyperscanning research using functional Near Infrared Spectroscopy (fNIRS) has shown that interpersonal coordination of frontal-lobe activity in specific time scales (3.2–12.8 s) is different in cooperative *vs* competitive interactions (Cui *et al.*, 2012). In such cases, the time durations (and, inversely, frequencies) with which events and processes unfold are examples of temporal scales.

However, what is important is that methods for examining change in coordination over time and/or studies that employ them are limited. To address this gap, we present and demonstrate an underutilized bivariate time series method we refer to as windowed multiscale synchrony (WMS). This method is a generalization of a phase synchronization methodology that was introduced to measure synchrony in noisy, non-linear time series typical of those from physiological or interpersonal measures (Schmidt *et al.*, 1990; Schmidt and O'Brien, 1997; Rosenblum *et al.*, 1998; Tass *et al.*, 1998; Dumas *et al.*, 2011). Methods, like the one demonstrated below, allow researchers to move beyond aggregate measures of coordination, providing a lens to focus on how the relative strength of coordination changes over the time scales that comprise social interaction (Gorman *et al.*, 2016). Further, it captures a different form of synchronization than other time- and frequency-varying measures such as phase coherence, which are correlation-based and sensitive to variations in amplitude (see section Comparison of WMS with Phase Coherence Results for additional details). More specifically, the advantage of the WMS method compared with other methods for examining synchrony is that it is sensitive to both 1:1 and n:m (i.e. other phase ratios) phase-locking dynamics that can be short in duration, time varying, and scale specific; WMS is robust to the influence of noise and non-covarying amplitude fluctuations.

WMS

WMS is a time and frequency decomposition-based technique based on the continuous wavelet transform. In brief, WMS measures the degree of coordination between two signals of equal length at each point in time across many frequencies. In other words, WMS provides a continuous synchrony index (SI) over time and across scales. As noted above, WMS is a generalization of a method for detecting phase synchronization in noisy and non-stationary bivariate time series data (Tass *et al.*, 1998). Those authors developed the method with neurophysiological measurements as a target application. WMS generalizes the Tass *et al.* (1998) method by investigating synchrony at many time scales simultaneously. The original method, being based on the Hilbert transform, only measures a single frequency at each moment in time Note, however, that the Hilbert transform when combined with band-pass filtering could be conducted to resolve synchrony at multiple frequencies/time scales (Le Van Quyen *et al.*, 2001). Phase synchronization, also known as phase locking, reflects the degree to which two oscillators have a constant phase difference or relative phase over some period of time, and measures of relative phase have figured prominently in both intra- and interpersonal coordination literature for many years (Haken *et al.*, 1985; Kugler and Turvey, 1987; Schmidt *et al.*, 1990; Amazeen *et al.*, 1998; Kurz and Stergiou, 2002; Richardson *et al.*, 2007 2012; Frank *et al.*, 2012; Washburn *et al.*, 2019).

However, in noisy and non-stationary time series, phase slips (rapid deviations from the current relative phase value) often make detection of synchrony difficult. To address this issue, Tass *et al.* (1998) approached the problem of measuring synchrony from a statistical perspective. Rather than focusing on a point estimate such as mean relative phase, they focused on the distribution of relative phase values where peaks in the distribution are informative regarding dominant phase differences (i.e. stable coordination patterns). Hence, the method detects synchrony even when there are sudden deviations in relative phase values or stable coordination patterns that are not clearly in-phase or anti-phase.

To quantify n:m phase synchronization, Tass *et al.* (1998) proposed two methods, only one of which is reviewed here. The method entails the following steps: (i) calculate instantaneous phase of each time series using the Hilbert transform, (ii) calculate the instantaneous relative phase between the two signals by taking their difference, mod 1, and (iii) compare the distribution of instantaneous relative phase values to a uniform distribution by calculating a measure of negentropy (based on Shannon entropy). This measure is normalized by dividing by the natural log of the maximum number of bins and subtracting that value from the entropy calculation. This essentially creates a normalized negentropy or SI that ranges from 0 to 1, with 0 indicating a uniform distribution (i.e. no synchrony), and 1 corresponding to perfect synchrony. Because this measure reflects the clustering of relative phase angles, it will show a high SI for unimodal as well as multimodal distributions (Hurtado *et al.*, 2004).

Much like the aforementioned aggregate coordination measures, this method too results in only a single phase synchrony

value. In other words, this scalar measure carries the tacit assumptions that synchrony is fixed to a single time scale and remains constant over time, both of which may be unreasonable in the context of individual and interpersonal physiology. Hence, Tass *et al.* (1998) proposed making repeated measurements of SI using a sliding window approach, providing the ability to observe time-varying patterns of synchrony (Hurtado *et al.*, 2004; Lai *et al.*, 2006). However, on its own, the sliding window approach only addresses one of those assumptions (i.e. time constancy). To address the second assumption, others have further extended the method via a continuous wavelet transform (Bocian *et al.*, 2018; Soczawa-Stronczyk *et al.*, 2019). A more detailed description appears below, but the basic idea is that the wavelet transform captures instantaneous phase at many different frequencies (or, inversely, scales), thereby allowing for measurements of synchrony at multiple frequencies. In the following paragraphs, we elaborate on the steps involved in this extension. MATLAB code for this procedure will be made available on the first author's github page (https://github.com/aaronlikens/wms).

Apply Morlet wavelet transform to decompose two time series into their component frequencies and calculate phase angles

Approachable, yet detailed introductions to the wavelet transform for both general use and for interpersonal coordination specifically can be found elsewhere (Cohen, 2014; Issartel *et al.*, 2015; Torrence and Compo, 1998). The wavelet transform refers to a family of methods that perform time-frequency decomposition of non-stationary signals, in the sense that they have time-varying frequency characteristics. It is based on a 'template matching' procedure between each time point in the observed signal and the template wavelet (Cohen, 2019). More technically, the wavelet transform involves time convolution between a signal and a wavelet (i.e. a small wave). The Morlet wavelet, a complex valued wavelet with both a real and imaginary component, allows for extraction of both instantaneous amplitude and phase of the observed signal (Issartel *et al.*, 2015). Constructing a Morlet wavelet involves pointwise multiplication of a Gaussian window and a complex sine wave:

$$wave = e^{i2\pi f} \tag{1}$$

where i is the imaginary number, f is peak frequency in Hz of the wavelet, and t is time. The Gaussian window is defined as:

$$GaussWin = ae^{-\frac{(t-m)^2}{2s^2}} \tag{2}$$

where a is the height of the Gaussian, t is time, m is an x-axis offset and s is the standard deviation of the Gaussian (Cohen, 2014). Importantly, s is defined as:

$$s = \frac{n}{2\pi f} \tag{3}$$

where f is the frequency in Hz, and n is the number of wavelet cycles and controls the trade-off between time and frequency precision. Small n emphasizes temporal precision at the cost of frequency precision; large n emphasizes frequency at the cost of temporal precision. A complete wavelet transform involves repeating the convolution for several values of f. In the present case, we used the following equation to determine the number of frequencies to resolve as $f = \text{floor}(\log2(T)\text{-}1)*12$, where T is the length of the series in question (Ashenfelter *et al.*, 2009). The product of the complex wavelet transform, then, is a time-frequency matrix of complex wavelet coefficients that represent estimates of the instantaneous amplitude and phase angle Φ, the latter of which ranges from $-\pi$ to π (Cohen, 2014). While not strictly part of the wavelet transform, after performing the wavelet transform on the two signals separately, the next step is to calculate the phase difference between each of the respective phase angle estimates ($\Phi = \Phi_1 - \Phi_2$) at each frequency and each movement in time.

Utilize WMS index for two signals to derive a continuous measure of phase synchronization

Following the wavelet transform and phase difference calculation of the two signals, one can calculate WMS at each frequency. That is, for each consecutive window at each frequency scale, the normalized negentropy calculation described above is computed. That is, the time frequency synchronization index (SI) is defined as

$$\tilde{\rho}\,(t,f) = \frac{S(t,f)_{max} - S\,(t,f)}{S(t,f)_{max}} \tag{4}$$

where

$$S\,(t,f) = -\Sigma_{k=1}^{N} p_k \ln p_k = \tag{5}$$

is the Shannon entropy of the relative phase distribution determined at each t and f using a sliding window. Here, N refers to the number of bins, which we define following the recommendation of Le Van Quyen *et al.* (2001) as $N = e^{0.626+.4\ln(M-1)}$, where M is the sliding window size. Note that the number of bins is fixed for f and the boundaries of the histogram should be set for consistency with the modulus operator used (e.g. mod 1 in this case). Hence, the interval [0, 1] should be divided into N bins, where N is derived from the above equation. Based on the simpler method that uses the Hilbert transform method (Tass *et al.*, 1998; Le Van Quyen *et al.*, 2001), $\tilde{\rho}(t, f)$, which from here on is referred to simply as the SI, ranges from 0 to 1 and depends on both time and frequency. Additionally, for a given window of relative phase values, we also extract the mean relative phase value, in order to provide information complementary to strength of the synchrony assessed, namely the typical phase relationship for a given window and frequency.

To better illustrate this SI measure, the example histograms shown in Figure 1 (which draw from frequencies of Simulation Experiment 1, details below) showcase how more uniform distributions (Figure 1 right) exhibit low values of SI, because there is not a stable coordination pattern. Figure 1 left, however, shows high SI when there is a unimodal distribution.

Applying this method requires the researcher to make parameter choices, including wavelet length and the minimum and maximum number of cycles in the wavelet, window size, minimum and maximum frequencies to resolve, and the number of frequencies in between. Making these choices entails theoretical and practical considerations.

In selecting window size, the researcher should select a window that is large enough to capture the expected dynamics of the series in question. This has consequences for frequency selection as well (see below). Ideally, the window should capture a few cycles of the behavior of interest. Additionally, because we calculate a form of Shannon entropy on the distribution of relative phase values, windows should contain sufficient data to

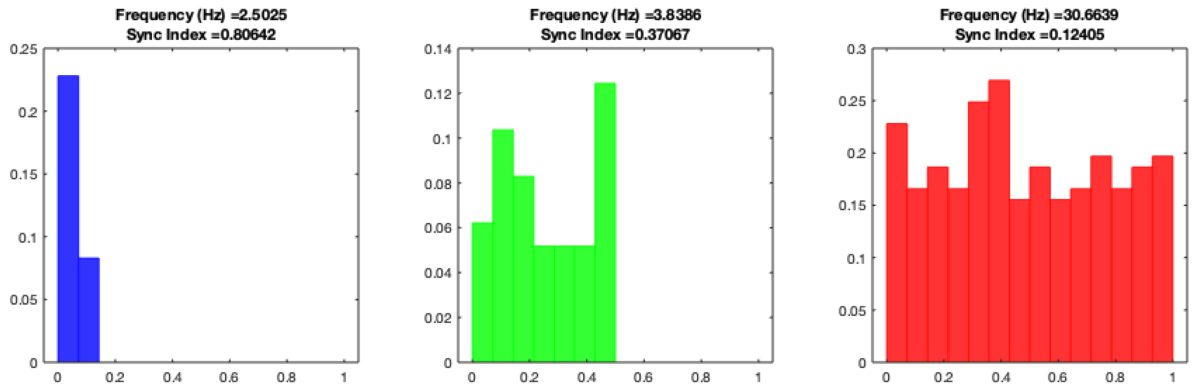

Fig. 1. Example histograms of mod 1 relative phase values where the left plot shows high SI, middle plot shows medium levels of SI and the right plot has a low SI.

obtain a stable estimate of entropy. Assuming a uniform distribution of phases, we suggest including >100 data points in each window. Windows much smaller than this may produce biased entropy estimates. Such windows are generally not an issue for physiological and movement data, which typically have high sampling rates (e.g. >50 Hz). Note also that it is common in windowing procedures to select window increments and window overlap. However, while these could be implemented in this method, to preserve the fine grained time resolution, we utilized a windowed increment value of 1 (thus, also an overlap of window size M−1).

Concerning the range of *f*, as many well versed in time-frequency analysis know, one cannot use frequencies higher than the Nyquist frequency, which is one-half the sampling rate of the signal. This does not mean that all possible frequencies below that extreme need to be analyzed. Instead, we suggest only investigating frequency ranges that are motivated by theory, previous research, and even findings in other modalities (cf. Wang *et al.*, 2020). For instance, many devices such as those used for motion capture or physiological measurements (e.g. electrocardiogram, electroencephalogram, and electromyogram [ECG], electroencephalogram [EEG], electromyogram [EMG]) have very high sampling rates (e.g. 1000 Hz). However, frequency content at 500 Hz or even 100 Hz may not be meaningful. Time-frequency methods like WMS can be computationally intensive. Hence, researchers should consider a more focused sub-range of frequencies relevant to their research questions, and whenever possible, frequency ranges should be based on theory or previous research.

Evaluate SI values relative to surrogate time series

As with many time series methods, it is important to statistically compare the observed SI values with those values generated from surrogate series. There are many options for generating surrogate time series to which to compare the observed SI values (Kantz and Schreiber, 2003; Hurtado *et al.*, 2004; Moulder *et al.*, 2018). For WMS, we generate a number of randomly shuffled permutations of each pair of time series and perform steps 1 and 2 above on each surrogate pair (for all of our examples below we used 19 randomly shuffled permutations; Kantz and Schreiber, 2003). From the surrogate SI values, 95% confidence intervals are generated for each point in the SI matrix, which are used to threshold and suppress all original SI values that fall within these bounds. Thus, any remaining SI values are greater than would be expected due to random chance (i.e. statistically significant).

Simulated data for testing WMS method

Two simulation experiments were conducted to investigate the performance of WMS. Our simulation experiments were designed with the following considerations: (i) time series should exhibit (at least) quasi-periodic behavior in one or more frequency bands; (ii) time series should have superimposed noise in order to emulate noisy measurement devices or biological noise commonly observed in laboratory experiments and naturalistic data collection; and (iii) each simulation should introduce a perturbation (e.g. a drop in a common frequency or sudden addition of matching frequency content), potentially capturable by WMS. To that end, we selected two systems that varied in terms of simplicity. Simulation Experiment 1 (SE1) involved a simple pair of harmonic oscillators, while Simulation Experiment 2 (SE2) involved a Rössler system coupled to a harmonic oscillator (Rössler, 1976; Stepp and Turvey, 2010, 2015). Specifics on those systems are provided below. WMS was then performed on each system to identify the degree of synchrony as well as the presence of the perturbations.

Simulation experiment 1: composite sine waves

As a baseline demonstration of WMS, we simulate two composite sine waves, x(t) and y(t), where time, t = 0.01, 0.02, 0.03, …, 60.00. Hence, x(t) and y(t) simulate recording a periodic system with two components for 1 min at a sampling rate of 100 Hz. Where x(t) and y(t) are defined in equations (6) and (7) as:

$$x(t) = \sin(2\pi 3t + \pi/3) + \sin(2\pi 0.5t) + \sin(2\pi 0.05t) \quad (6)$$

$$y(t) = sin(2\pi 3t) + \sin(2\pi 1t) + \sin(2\pi 0.5t) \quad (7)$$

and for t = 7 − 20.50 s

$$y(t) = y(t) + sin(2\pi 0.05t)$$

These simulated sine waves show that x(t) has a constant 3 Hz signal that is shifted by $\pi/3$, a constant 0.5 Hz, and a constant 0.05 Hz component, while y(t) has a constant 3 Hz component (not shifted), 1 Hz, and 0.5 Hz, as well as a 0.05 Hz component added between t = 750 (14 s) and 2050 (21 s). Next, unique sources of Gaussian noise (zero mean and unit variance) were added to x(t) and y(t), respectively. Figure 2 (top-left) depicts these noisy composite sine waves. As noted earlier, WMS requires specification of several parameters related to the wavelet transform and windowing procedure. For this

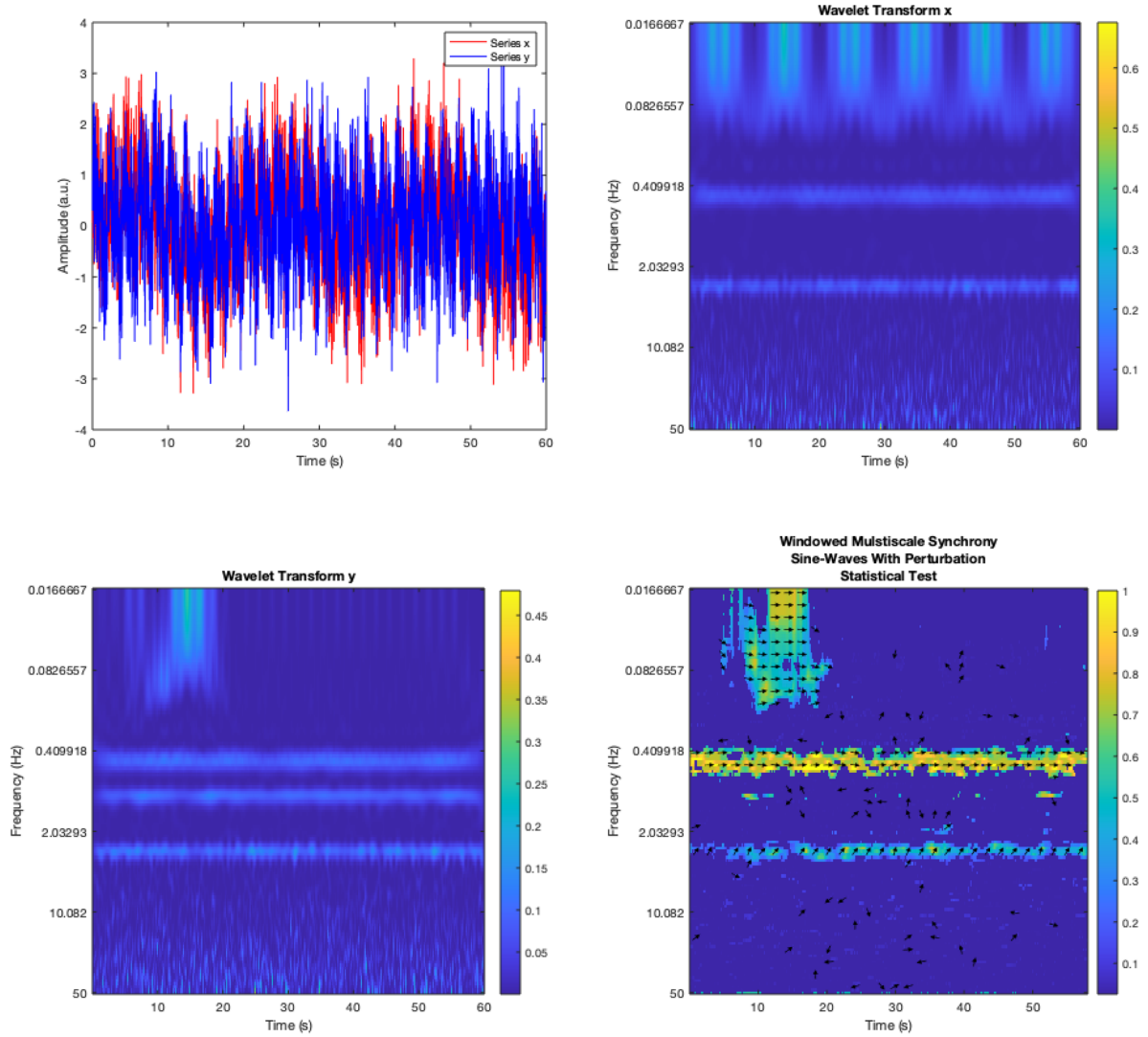

Fig. 2. Top-left of the figure shows the two composite sine wave series with noise added as described in equations (6) and (7). Top-right and bottom-left show the frequency spectrum of the wavelet transform for series x and y respectfully. Bottom-right shows the results of applying WMS to series x and y.

experiment, we used the following wavelet parameters: (i) a Morlet wavelet with 5 to 8 cycles, (ii) wavelet length = 4 s, and (iii) a sliding window length of 2 s.

The expectation for this experiment was that WMS would reveal the expected phase-locked behavior at 3 and 0.5 Hz, which would be evident from relatively larger SI values at that frequency. An additional expectation was that WMS would uncover an increase in the SI during seconds 7 to 20.50 due to the imposed perturbation. Evidence for this would be a sudden increase in synchrony at 0.05 Hz during that time period. Lastly, WMS would not reveal any consistent patterns of synchrony outside of the simulated matching frequency bands with the exception that there would be some frequency smearing.

Simulation experiment 1 results

Figure 2 (top-right and bottom-left), shows the wavelet transform of series x(t) and y(t), respectively and depicts the expected dominant frequencies within these signals (i.e. 0.05, 0.5, 1 and 3 Hz). WMS results appear in Figure 2 (bottom-right), and support all three expectations reported in the preceding paragraph. First, WMS provides evidence that x(t) and y(t) maintain a nearly constant relative phase over time for the 0.5- and 3-Hz components and these are greater than the surrogate threshold. Second, WMS captures the expected rise in synchrony of x(t) and y(t) during the time period marked by the perturbation at 0.05 Hz. Third, the relative phase arrows clearly capture the expected pattern in which most of the arrows indicate in-phase relationships, but for the 3 Hz band, the relative phase is shifted. Lastly, WMS suggests the presence of synchrony centered around the frequency ranges anticipated from equations (6) and (7).

Simulation experiment 2: coupled system dynamics

As a second demonstration, we examine the performance of WMS on a coupled dynamical system composed of a Rössler equation (Rössler, 1976) and a harmonic oscillator:

$$x_1' = -x_1 - x_3 \tag{8}$$

$$y_2' = y_2 + k\left(x_1 + y_{1,\tau}\right) \tag{9}$$

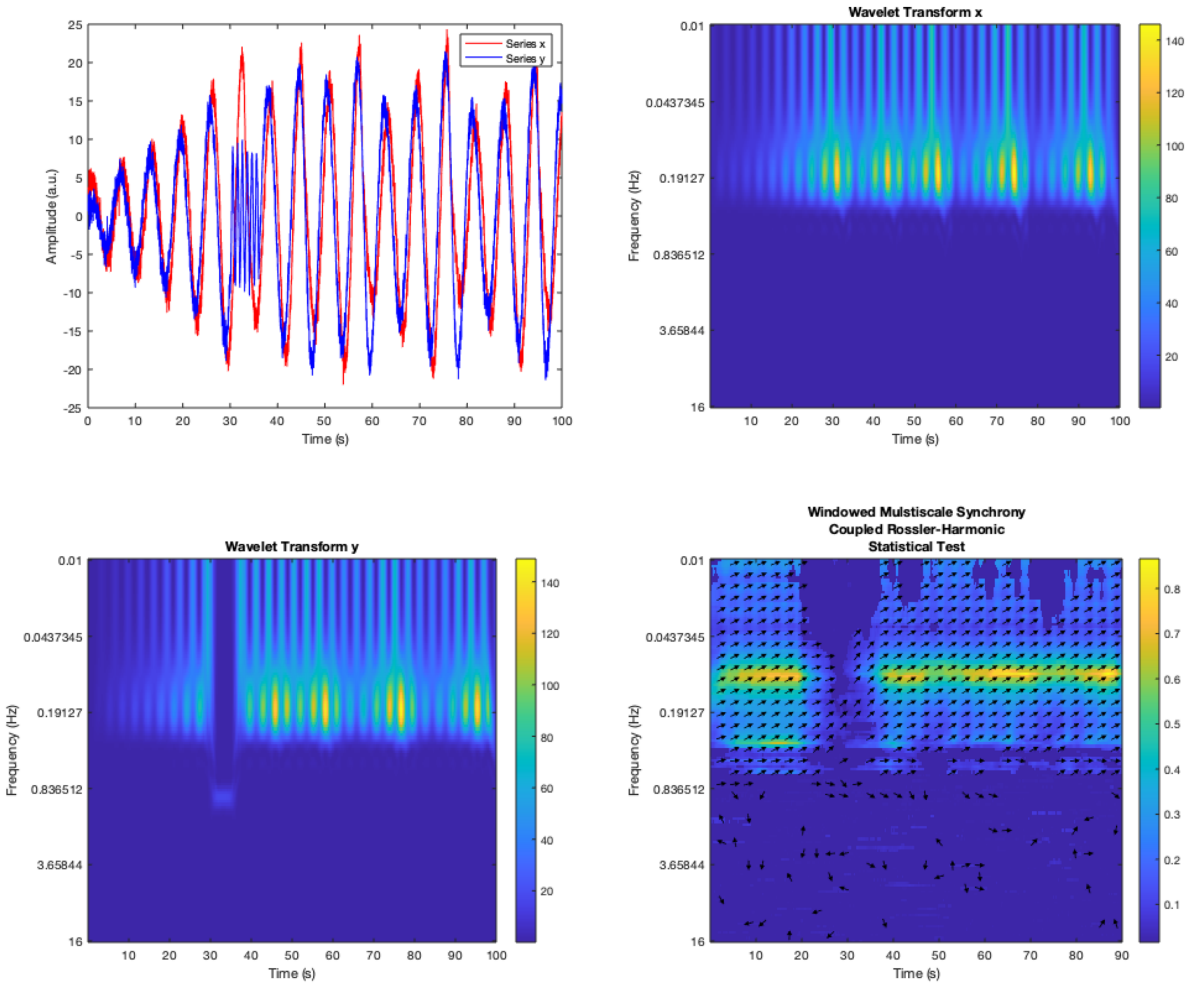

Fig. 3. The top-left graph shows the time series plots of the Rössler and harmonic system that were delay coupled as indicated in equations (8) and (9), respectively. Top-right and bottom-left show the frequency spectrum of the wavelet transformed series. The bottom-right graph shows results of the WMS analysis with surrogate thresholding.

where equation (8) represents a chaotic Rössler oscillator and equation (9) represents a simple harmonic oscillator that is unidirectionally coupled to equation (8) (Stepp and Turvey, 2010 2015). Note that the ‘’ symbol indicates that the variables on the left side of both equations are the first derivative, τ indicates a time delay and k reflects coupling strength. This configuration represents an instance of delay coupling, which produces anticipating synchronization wherein a driven system anticipates future states of a driving system. These and similar systems have been discussed at length in papers dealing with strong anticipation, which has been posited as a general mechanism underlying coordination in systems ranging from pairs and populations of neurons to coordination of groups of people (Stepp and Turvey, 2010, 2015; Dalla Porta *et al.*, 2019; Washburn *et al.*, 2019). A complete description of anticipating synchronization is beyond the scope of this paper (but see the above references for excellent introductions); however, there are several key dynamic properties such systems exhibit that are useful for testing the behavior of WMS.

Similar to the series used in SE1, the series used in SE2 are also oscillators; however, several key dynamics make SE2 a more realistic test of the WMS method. That is, these delay coupled systems permit additional hypotheses that are perhaps more reasonable in the context of interpersonal coordination experiments. First, systems that develop anticipating synchronization are attracted to a consistent phase lag such that the driven system begins to anticipate (i.e. phase lead) the driver over time. Hence, a reasonable hypothesis is that WMS will reveal a consistent pattern of synchronization over time. Second, altering the dynamics of one of the time series should interrupt this consistent pattern resulting in breakdown in synchronization.

These hypotheses were explored by simulating the coupled system according to equations (8) and (9). Next, unique sources of Gaussian noise were again added to each component of the coupled Rössler and harmonic series. Thus, these series simulate recording a delay coupled system for 100 s at a sampling rate of 50 Hz. Figure 3 (top) depicts examples of these series. Similar to the procedure in SE1, we introduced a perturbation by modifying seconds 30 to 36 of the harmonic oscillator to exhibit an uncoupled, dominant 1-Hz frequency. Again, this was done to examine WMS ability to capture perturbations to synchrony. The wavelet parameters used in SE2 were the same as those in SE1.

Simulation experiment 2 results

Results from this experiment are captured in Figure 3. Figure 3 (top-left) visualizes the time series that is useful for interpreting

the WMS results depicted in Figure 3 (bottom-right). Figure 3 (top-left) shows that, as expected, the system tends toward a phase lead pattern indicative of anticipating synchronization and the phase arrows taken in tandem with the SI values in the bottom-right support this intuition. Phase arrows pointing to the right and parallel to the horizontal axis indicate in-phase; phase arrows pointing to the left that are parallel to the horizontal axis indicate anti-phase behavior. Deviations from those extremes indicate phase lead and lag. Note how the harmonic oscillator tends to reach its peaks in time earlier than the Rössler oscillator, regardless of the instantaneous frequency. Note also that the obvious perturbation near 30 s when the harmonic oscillator switches to a constant frequency of 1 Hz.

Focusing now on the results from the WMS analysis, there is evidence to support our hypotheses. As noted above, there are high SI values ($\sim$ >0.60) around 0.1 Hz that exceed the surrogate threshold and the shifted relative phase arrows show evidence of anticipating synchronization. There is also clear evidence of change in synchrony over time that follows consistent with the applied perturbation. This is evident in the 0.1-Hz region between 25 and 35 s where the SI values become lower than the surrogate threshold.

Physiological data set for demonstrating method

Next, we evaluate the WMS method on an openly available ECG data set collected as part of an evaluation of collaborative cognition in a 1-hour paired-programming classroom setting (Ahonen *et al.*, 2016). We selected this data because the originating author found evidence of a form of synchrony between 19 student dyads during this task and the data were freely available. The ECG data were collected using a medical grade ECG device sampled at 500 Hz. In this case, WMS is a relevant analysis because ECG data are commonly analyzed in terms of heart rate variability and are typically decomposed into multiple psychophysiologically meaningful frequencies that can change over time (Hoover *et al.*, 2012).

While full details of the participants and study design can be found in the primary source (Ahonen *et al.*, 2016), here we describe the task in more detail to facilitate understanding of our WMS results. The dyadic paired-programming task involved student programmers in a classroom setting with little programming experience. Each pair worked on standard programming tasks from the curriculum at a shared workstation (i.e. a single computer). The first 7 min of the task involved watching a video. For the remainder of the approximately 1-hour period, participants alternated task roles every 7 min. One participant was the 'driver' in which they were actively doing the programming. The other participant was a 'navigator' that observed and provided comments and guidance on the task.

Physiological data example: HRV

We preprocessed the ECG and calculated the IBIs using the Colibri package (Henelius, 2016) for R (R Core Team, 2018) and the script detailed in Ahonen *et al.* (2016). Computing any form of synchrony (e.g. cross-correlation) presents a special challenge in the case of IBI time series because heart rate varies considerably over time and no two heart rate series will be identical (Goldberger *et al.*, 2002). This is problematic because IBI series from individual members of a dyad will ultimately have differing lengths. To remedy this issue, we time normalized each IBI series by resampling the original time series using linear interpolation into equally spaced, half-second intervals, from the first time stamp of the later starting time series until 3600 s (Spivey and Grosjean, 2005). Figure 4 top-left visualizes an example pair of time-normalized IBI series. This effectively resamples the IBI series at 2 Hz as has been done in prior research (Golland *et al.*, 2015; Bizzego *et al.*, 2020) in which linear interpolation was shown to have better performance for time-domain and high-frequency variability compared with other interpolation measures (Choi and Shin, 2018). Heart rate variability measures, typically extracted from the IBI series, are parsed into the following frequency bands: ultra-low frequency ($\leq$ 0.003 Hz), very low frequency (0.0033–0.04 Hz), low frequency (0.04–0.15 Hz), and high frequency (0.15–0.4 Hz) (Shaffer and Ginsberg, 2017). Our WMS parameters for this analysis were as follows: (i) a Morlet wavelet with 5 cycles, (ii) wavelet length = 1750 s, and (iii) a sliding window length of 150 s (or 300 data points) with a focus on frequencies between 0.003 and 0.4. This range was selected because we cannot resolve any frequencies in the ultra-low frequency range due to requiring 24 hours' worth of data (Shaffer and Ginsberg, 2017).

HRV example results

Figure 4 shows exemplar WMS results for the IBI time series of one dyad (see bottom right). Generally, there is evidence of synchrony (see Figure 4, bottom-right), such that, after surrogate testing, primarily only very low frequencies display stronger interpersonal synchrony (< 0.007 Hz) with values that are close to SI = 1 for extended periods with phase arrows that vary considerably from one bout of synchronization to another. It is worth emphasizing, that in comparison to the previous examples, the time scale is much longer for these data, so not only are there large magnitude SI values, but they do also have a tendency to remain high for at least a couple minutes before dissipating and recurring at later time points (e.g. 10–17 min, $\sim$ 25–30 min periods). In addition, these drift patterns sometimes traverse several neighboring frequencies or frequencies ranges that are far apart (for example, 0.003 and 0.006 Hz around $\sim$ 25–30 min). Note that while there are large portions of the plot that do not appear to show high SI values, we include this full range of justifiably interesting frequency ranges for heart rate variability (HRV). This, in turn, illustrates one of our key claims that aggregate measures of interpersonal coordination do not always capture the ways that people move in and out of synchrony over time. Synchrony can be very strong and specific to certain spatiotemporal scales, while non-existent in others.

Neuromechanical data set for demonstrating method

For our final demonstration of the WMS method, we utilize another openly available dyadic postural sway data set (Okazaki *et al.*, 2015). Postural sway, which characterizes the ability to maintain upright posture, is argued to be neuromechanical as it reflects the complex interactions of the nervous and the musculoskeletal systems (Ting and Allen, 2013). In their study, Okazaki *et al.* (2015) investigated interpersonal synchrony in postural sway where 22 dyads were instructed to stand and look at each other during 60s trials while minimizing movement and thinking only about the other participant. Across 32 trials, participants either stood far away (70 cm) or near (20 cm) and had

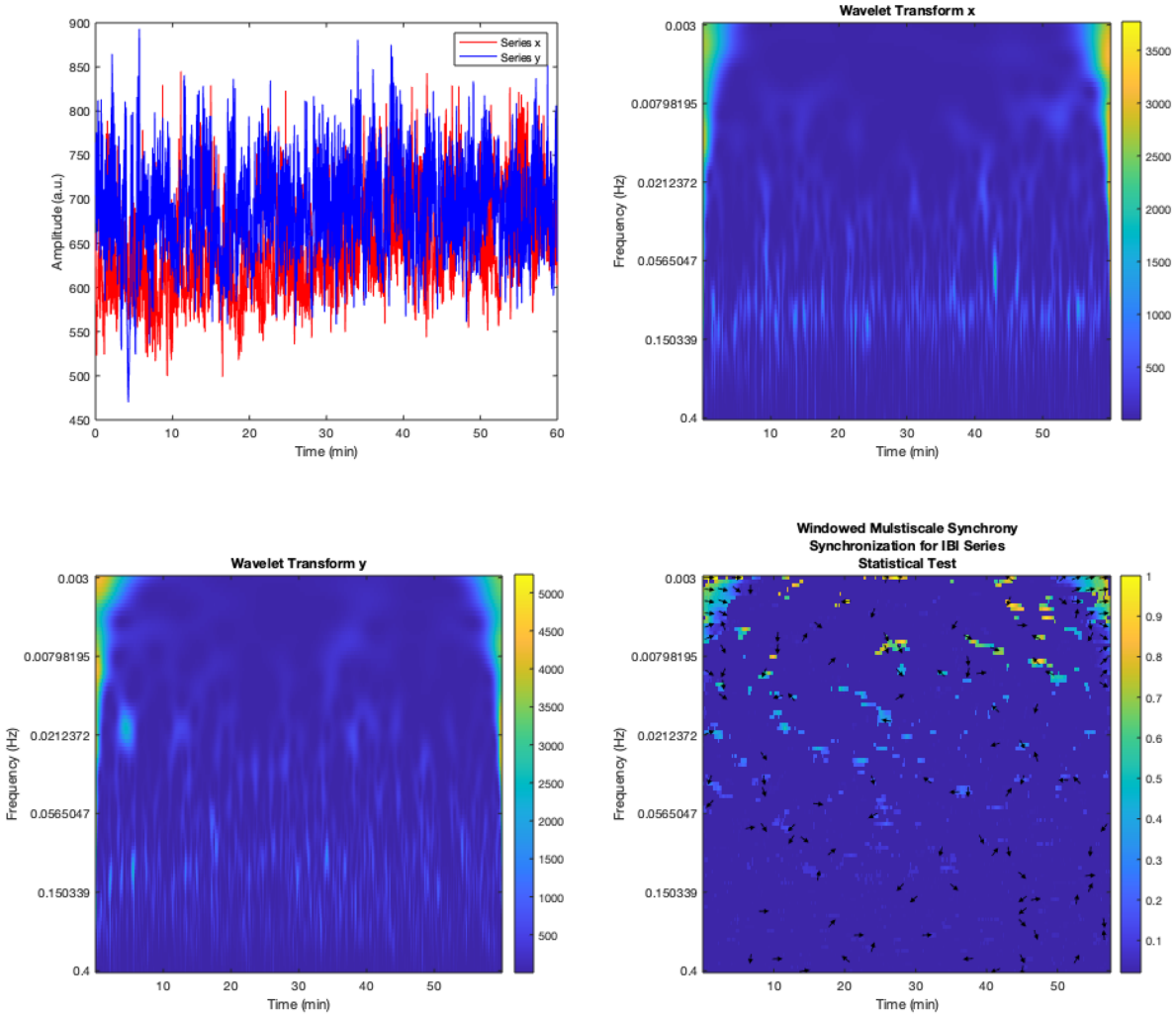

Fig. 4. Top-left of the figure shows two time-normalized IBI series. Top-right and bottom-left show the frequency spectrum of the wavelet transform for the two series. Bottom-right shows the results of applying WMS to the IBI series with surrogate thresholding.

reciprocal visual information (both participants could see each other), no visual information (both participants wore blindfolds), and partial visual information where one of the participants wore a blindfold and the other did not. Participants took turns being blindfolded.

Postural sway was captured using an infrared-camera based motion capture system that detected five markers on glasses that participants were required to wear (full details can be found in the original manuscript). The markers were used to calculate the head position of each participant and their movement along the anterior–posterior (AP; front-back movement) and mediolateral (ML; left-right movement) directions at a sampling rate of 200 Hz. This data set was Selected because the authors found evidence of postural sway synchrony using time-lagged cross-correlations where synchrony was strongest for those in the reciprocal visual information condition and because postural sway is known to depend on multiple time scales (Collins and De Luca, 1993; Likens *et al.*, 2019). Our WMS parameters for this analysis were as follows: (i) a Morlet wavelet that varied between 3 and 20 cycles from lowest to highest frequency, (ii) wavelet length = 4 s, and (iii) a sliding window length of 2 s (or 400 data points) with a focus on frequencies between 0.005 and 100 Hz.

Neuromechanical example results

For our analysis of the postural sway data, we focus on the movement data along the ML axis for one pair of participants in each visual information condition described above, but only for the near condition (which showed the highest synchrony on average). Figure 5 top shows an example pair of time series for the two participants from the reciprocal visual information condition. The bottom four plots show the WMS results on the postural sway data from the four different visual information conditions. All of the conditions show evidence of synchrony beyond the surrogate thresholds in the 0.02- to 0.5-Hz range. A surprising observation is that, contrary to the original findings, the no visual information condition (Figure 5 middle-right) shows evidence of synchronization on par with the full visual information condition (middle-left); (Okazaki *et al.*, 2015). That is, there is relatively consistent, in-phase synchrony for both conditions across the 1-min trial. In contrast, the partial visual

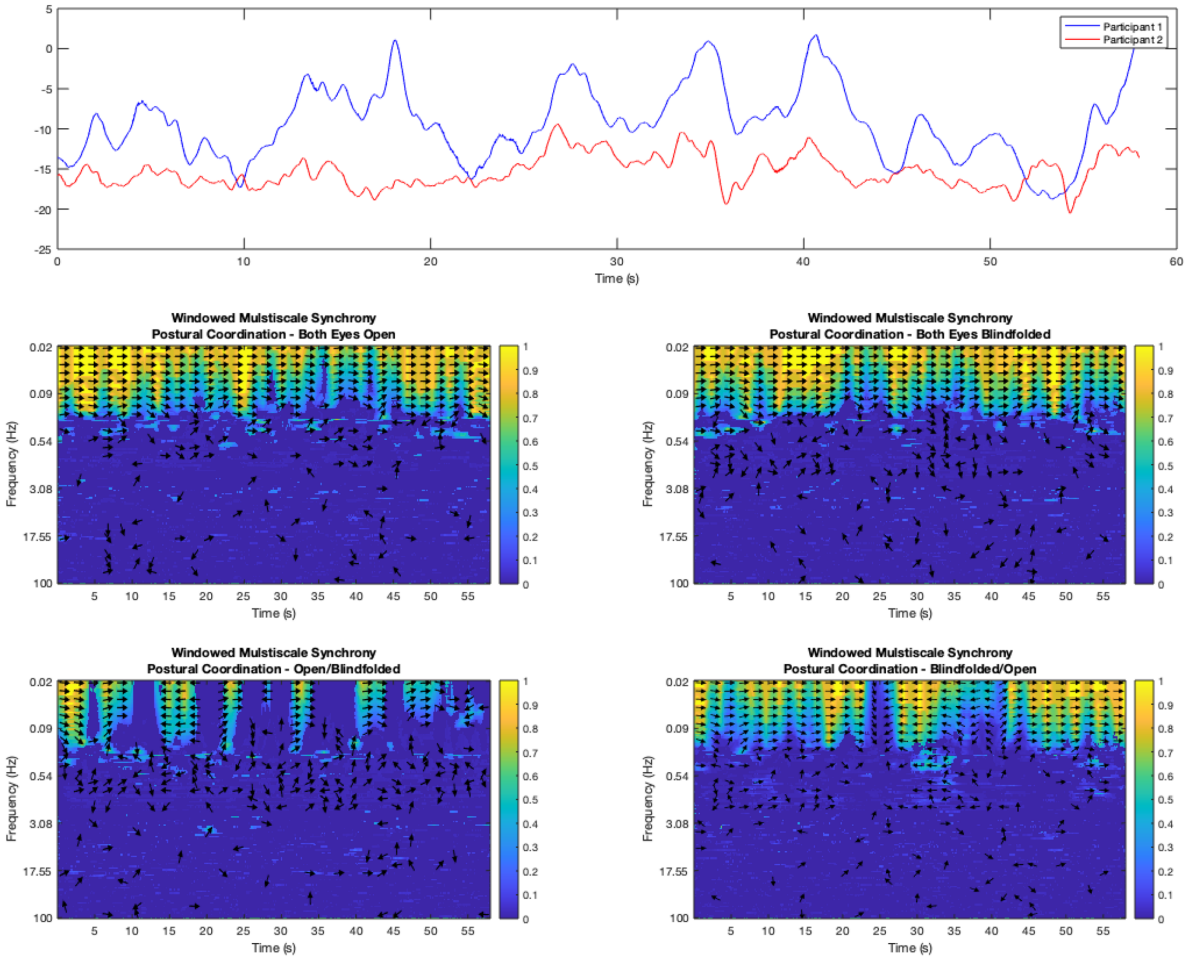

Fig. 5. Top shows two example postural sway time series for a dyad from the Okazaki *et al.* (2015) data set. Middle-left and middle-right show WMS results from a single dyad with both participants' eyes open and both participants' eyes closed, respectively. Bottom-left and bottom-right show WMS results from a single dyad where only one of the participants is blindfolded and the other has eyes open.

information condition implies patterns similar to the original findings, in that there seems to be a strong asymmetry in synchrony, depending on which partner had visual information. When Participant 2 had visual information, synchrony seems to be greater with more consistent relative phase over time. Not only this, but when Participant 1 had visual information, the synchronization was intermittent with alternating patterns of in-phase and anti-phase coordination.

Comparison of WMS with phase coherence results

While a comparison of WMS with the many possible methods for examining synchrony (Quiroga *et al.*, 2002; Butler, 2011; Delaherche *et al.*, 2012; Butner *et al.*, 2014; Schoenherr *et al.*, 2019) is beyond the scope of the paper, we do provide an example comparison here with one of the most closely related methods, time-dependent phase coherence, which Hurtado *et al.* (2004) defined as:

$$\gamma_{fM(t_k)} = \left| \frac{1}{N} \sum_{j=k-M}^{k} e^{i\Phi_{fj}} \right|^2 \tag{10}$$

In this case, equation (10) shows that for each frequency f, at teach time point t_k that terminates each window of length M, the phase coherence measure is applied to the same relative phase time series ($\Phi_{f,j}$) as is done in WMS.

This measure is more directly comparable to WMS than coherence computed from the cross-wavelet transform (CWT), for example, because it is less sensitive to variations in amplitude than 'a localized correlation coefficient in time frequency space' (p. 564; Grinsted *et al.*, 2004) would be and it is applied directly to the same relative phase series using the same windows (Hurtado *et al.*, 2004). The SI from WMS is based on the distribution of phase differences in a given window, and then the negentropy calculation is applied to that distribution. Nearly all correlation-based methods for examining synchrony are subject to variations in amplitude as well as phase. While the SI value, like coherence using the CWT, ranges from 0 to 1, instead of informing us of the covariance of the two signals, it informs us about the relative stability of the observed coordination pattern. That is, WMS can provide an answer to the question: do two signals exhibiting a particular relative phase relationship (values close to 1) or is each relative phase value equally likely to occur (values close to 0)? Entropy-based measures such as this have been used to examine neuro- and physiological synchrony in other work corresponding to changes in team coordination (Likens *et al.*, 2014; Amazeen, 2018) and in some cases have been more sensitive to synchrony than correlation-based measures (Strang *et al.*, 2014), while other work highlights convergence with many measures using EEG data (Quiroga *et al.*, 2002).

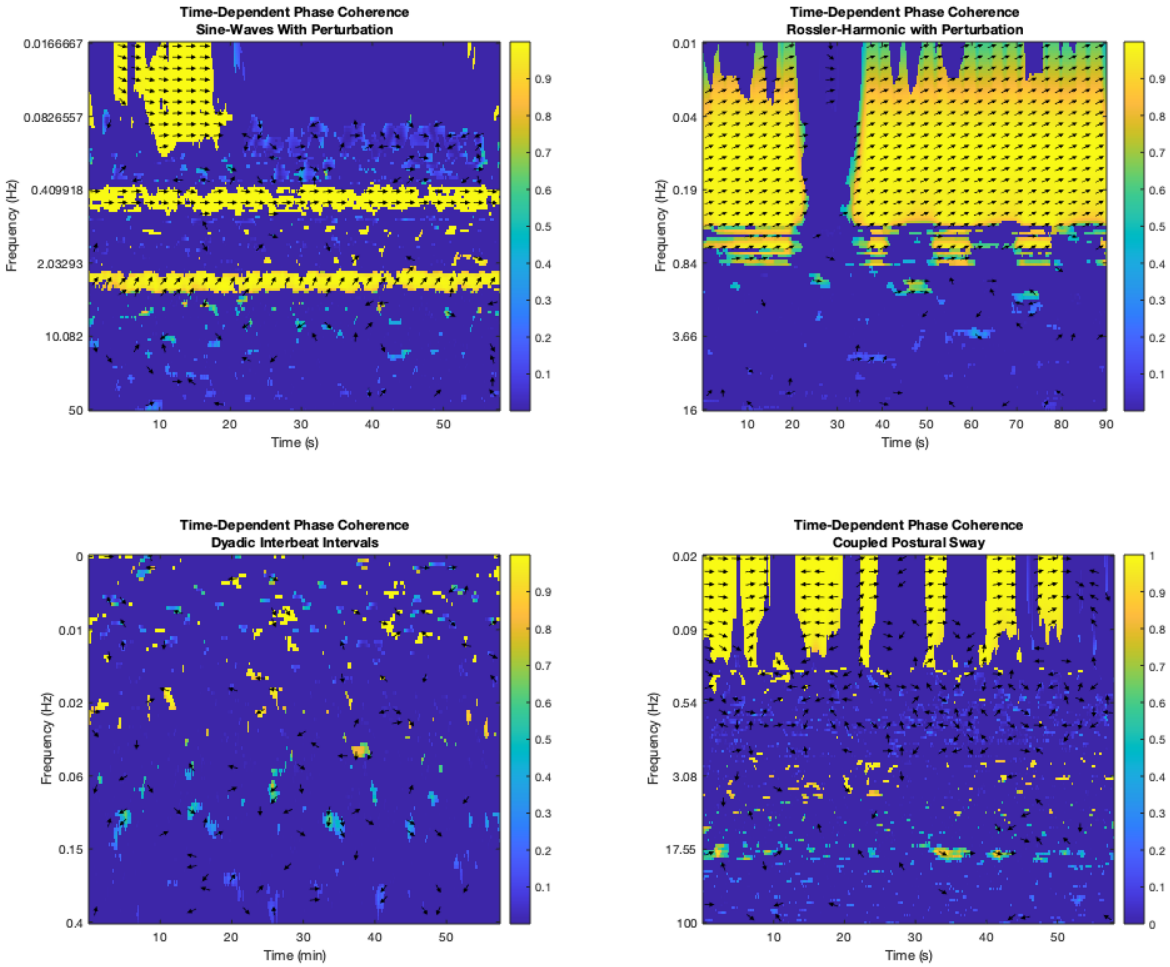

Fig. 6. Time-dependent phase coherence analyses applied to the composite sine wave example (top-left), Rössler system (top-right), paired programming IBI data (bottom-left) and the dyadic coupled postural sway data (bottom-right).

Whereas the time-dependent phase coherence used here is more sensitive to phase locking when the relative phase values are clustered around a single value, the negentropy-based SI is more sensitive to multimodal clustering (i.e. multiple stable relative phase values; Hurtado *et al.*, 2004). That being said, we apply the time-dependent phase coherence to each of the examples above. The plots shown in Figure 6 can be directly compared with the corresponding WMS plots. It is evident that these two measures provided largely convergent information for the majority of the cases, which was expected given their similarity (Hurtado *et al.*, 2004). However, there are also some noticeable differences. Time-dependent phase coherence produces greater frequency smearing and more indication of time-frequency regions with high coherence (i.e. over and above surrogate thresholds) than does WMS. Regarding the latter point, it seems that coherence values tend toward one—WMS values appear more variable, occupying more of the theoretical range between 0 and 1, possibly indicating that WMS is more conservative in detecting synchrony. This is perhaps most apparent with respect to the postural sway example, where The majority of significant coherence values in low frequency regions appear to be at ceiling, and there are also a number of significant coherence values in high frequencies (e.g. >17 Hz), outside of 10 Hz frequency cutoff typically investigated for postural control (Winter, 2009).

We chose one of the most similar measures with which to compare the negentropy-based SI because this time-dependent phase coherence shares many of the same properties. For instance, it allows one to look at phase-locking tendencies at multiple frequencies over time. Comparisons with aggregate measures such as correlation of HRV features, as well as cross-correlations of the postural sway data, can be found in original articles that originated the datasets we analyzed (Okazaki *et al.*, 2015; Ahonen *et al.*, 2016).

Discussion

This paper demonstrated the use of the WMS method on composite sine waves with multiple coordinated frequencies with a shift, coupled oscillators with anticipatory dynamics, physiological data derived from a paired programming task and, interpersonal postural sway data from a variety of visual information conditions. Taken together, we have shown that WMS provides a continuous SI over time and across frequency scales that not only shows the frequency/scales at which coordination takes place, but also how it changes over time. This is in contrast to many of the more established methods for measuring interpersonal synchrony such as cross-correlation and cross-recurrence quantification analysis. In our simulation examples, we see that

WMS depicts coordination transitions clearly and at relevant scales. The empirical analysis of the IBI data showed that certain scales exhibit coordination whereas others do not, and the coordination strength and scale tend to ebb and flow over time as well. In the postural sway data, the WMS results showed a general tendency for participants to synchronize their postural sway in the ML direction. In addition, WMS results revealed a strong directional dependence for the dyad we analyzed. In general, these results imply that WMS may be useful in a broad number of contexts involving interpersonal coordination dynamics.

A major aim of this paper was to simply educate researchers about the methodological considerations of WMS and to demonstrate its utility in the context of interpersonal coordination. This was done in hopes of inspiring new theoretical and methodological work. The remainder of the discussion highlights several research areas we consider promising in that regard.

Investigating WMS in other domains

Given the variety of systems demonstrated in the current work, a natural next step is to apply WMS in other experimental domains. An obvious application of WMS is in the context of neurophysiological data, such as EEG, particularly in hyperscanning situations. Moreover, while we demonstrated WMS on postural sway data, we also expect that WMS will reveal important insights about coordination among specific limb segments within and across participants. More generally, WMS may reveal patterns of coordination in the many domains entailed by interpersonal coordination dynamics, ranging from important dyadic relationships to synchronization in teams (Louwerse *et al.*, 2012; Palumbo *et al.*, 2017). Importantly, any such efforts should attempt to link the coordination patterns observed to relevant outcome variables (Miles *et al.*, 2017; Wiltshire *et al.*, 2019, 2020) or differentiating variables such as clinical diagnoses (Schilbach, 2019). As work in this area progresses, time- and scale-specific research questions and hypotheses can be generated, relating, for example, to learning and changes in coordination over time.

Comparing WMS to other methods

Naturally, WMS has similarities to other measures used to examine coordination between time series in either frequency or time domains. Because WMS relies on the wavelet transform and thus preserves time-frequency information, it is similar to wavelet cross-coherence (Grinsted *et al.*, 2004). A key difference though is that WMS focuses on time-varying synchrony over multiple frequencies established by examining the distribution of relative phase values, and cross-coherence emphasizes point estimation of relative phase values. In the current work, we have compared WMS to time-dependent phase coherence because of their inherent similarities in terms of windowing and robustness to variations in amplitude. A systematic comparison of WMS performance with other measures for examining coordination, such as recurrence-quantification-based methods (e.g. Wallot and Leonardi, 2018), cross-correlation (e.g. Boker *et al.*, 2002), wavelet cross-coherence (e.g. Issartel *et al.*, 2015), detrended cross correlation analysis/multiscale regression analysis (Likens *et al.*, 2019; Podobnik and Stanley, 2008) and vector autoregressive/error correction modeling (Engle and Granger, 1987), is beyond the scope of the current manuscript; we expect, however, that future work of such nature would be an important contribution to the literature (Schoenherr *et al.*, 2019).

Potential approaches for improving and generalizing WMS

The current work demonstrates that WMS has utility in several contexts, but no method is perfect and there are often a number of ways to improve performance of time series methods. For example, experimental research may require summarizing SI within specific time-frequency regions. To that end, WMS method may be treated like any other time-frequency analysis. As such, efforts to summarize WMS will benefit from existing approaches to information extraction in time-frequency plots (see Issartel *et al.*'s, 2015 section titled 'How to Extract Useful Information from a Time-Frequency Representation' for additional ideas), and will facilitate the use of common statistical tests related to particular events, stimuli, conditions, and/or time points.

Also warranted is a deeper evaluation WMS performance under varying noisy conditions, along with data from social interactions with/without clear transitions and perhaps even, social interactions with controllable virtual partners (Fairhurst *et al.*, 2013; Dumas *et al.*, 2014). With such data, wavelet ridge detection (Jha and Senroy, 2018), real-time change detection (Hoover *et al.*, 2012) and/or non-linear prediction error algorithms (Kantz and Schreiber, 2003; Gorman *et al.*, 2019) could be utilized for marking critical transitions in the observed coordination values. Applying these in such a multiscale fashion would also be novel and could potentially allow for detecting critical and meaningful changes in interpersonal synchrony.

Furthermore, there are opportunities to generalize WMS. A notable example is to translate WMS from a bivariate to a multivariate approach, perhaps following other approaches to multivariate phase synchrony (Richardson *et al.*, 2012; Shahsavari Baboukani *et al.*, 2019). This generalization would broaden WMS' applicability to understanding coordination in groups larger than dyads and in cases such as neurophysiology where there are many data streams. Lastly, wavelet-based methods, which are known to suffer from frequency smearing and edging effects, may be improved by incorporating synchrosqueezed transformations (Tary *et al.*, 2018), so this is also likely a worthwhile area of investigation for WMS as well.

In addition to the above considerations, another improvement would include exploring alternative algorithms for estimating entropy/negentropy. The present work and the original work by Tass *et al.* (1998) computed entropy based on the histogram method. While this method is standard in many contexts, the fundamental algorithm is known to be biased (Schürmann, 2004). Hence, a systematic investigation to compare the performance of the alternative methods for calculating entropy within multiple contexts would identify the contexts in which certain entropy methods perform well in and those that they perform poorly.

In the current work, we used a surrogation method that tested the white noise null hypothesis, but other null hypotheses will likely be useful such as a first-order autoregressive process or any number of higher order linear hypotheses (Kantz and Schreiber, 2003; Grinsted *et al.*, 2004). Furthermore, other methods of surrogation that do not assume an underlying noise process may be more appropriate when the psychological or physiological processes under investigation are known to produce pseudo-periodic patterns of behavior (Small *et al.*, 2001).

Future work should explore how other null hypotheses impact the sensitivity of WMS in detecting synchronization phenomena.

Conclusion

In conclusion, we have shown examples of WMS applied to two noisy simulated data sets as well as two interpersonal empirical data sets including a physiological and neuromechanical example. This method provides a continuous index of synchrony over time between two time series that can vary across frequency/scale. Therefore, it provides a methodological tool that allows one to examine not only the strength of interpersonal coordination, but also how that coordination changes over time and at which scales. We expect that in making WMS more accessible, developing it further, and applying it to more widespread domains, substantive theoretical advancements can be made in understanding the form and function of interpersonal coordination across contexts.

Acknowledgements

This work was supported in part by a Pilot Project Award made to A.L. by the National Institutes of Health and the Center for Research in Human Movement Variability.

Conflict of interest

None declared.

References

Abney, D.H., Paxton, A., Dale, R., Kello, C.T. (2015). Movement dynamics reflect a functional role for weak coupling and role structure in dyadic problem solving. *Cognitive Processing*, *16*(4), 325–32.

Ahonen, L., Cowley, B., Torniainen, J., Ukkonen, A., Vihavainen, A., Puolamäki, K. (2016). Cognitive Collaboration Found in Cardiac Physiology: study in Classroom Environment. *PLoS One*, *11*(7), 1–16.

Amazeen, P.G. (2018). From physics to social interactions: scientific unification via dynamics. *Cognitive Systems Research*, *52*, 640–57.

Amazeen, P.G., Amazeen, E.L., Turvey, M.T. (1998). Dynamics of human intersegmental coordination: Theory and research. In D. A. Rosenbaum & C. E. Collyer (Eds.),. *Timing of Behavior: Neural, Psychological, and Computational Perspectives*, 237–259. Cambridge, MA: MIT Press.

Ashenfelter, K.T., Boker, S.M., Waddell, J.R., Vitanov, N. (2009). Spatiotemporal symmetry and multifractal structure of head movements during dyadic conversation. *Journal of Experimental Psychology. Human Perception and Performance*, *35*(4), 1072.

Bizzego, A., Azhari, A., Campostrini, N., et al. (2020). Strangers, friends, and lovers show different physiological synchrony in different emotional states. *Behavioral Sciences*, *10*(1), 11.

Bocian, M., Brownjohn, J.M.W., Racic, V., et al. (2018). Time-dependent spectral analysis of interactions within groups of walking pedestrians and vertical structural motion using wavelets. *Mechanical Systems and Signal Processing*, *105*, 502–23.

Boker, S. M., Rotondo, J. L., Xu, M., King, K. (2002). Windowed cross-correlation and peak picking for the analysis of variability in the association between behavioral time series. *Psychological methods*, *7*(3), 338–355.

Butler, E.A. (2011). Temporal Interpersonal Emotion Systems: the "TIES" That Form Relationships. *Personality and Social Psychology Review*, *15*(4), 367–93.

Butner, J.E., Berg, C.A., Baucom, B.R., Wiebe, D.J. (2014). Modeling coordination in multiple simultaneous latent change scores. *Multivariate Behavioral Research*, *49*(6), 554–70.

Chanel, G., Betrancourt, M., Pun, T., Cereghetti, D., Molinari, G. (2013). Assessment of computer-supported collaborative processes using interpersonal physiological and eye-movement coupling. *Affective Computing and Intelligent Interaction (ACII), 2013 Humaine Association Conference On*, 116–22.

Choi, A., Shin, H. (2018). Quantitative analysis of the effect of an ectopic beat on the heart rate variability in the resting condition. *Frontiers in Physiology* Cambridge, MA, 9, 1–19,

Cohen, M.X. (2014). *Analyzing Neural Time Series Data: Theory and Practice*. Cambridge, MA: The MIT Press.

Cohen, M.X. (2019). A better way to define and describe Morlet wavelets for time-frequency analysis. *NeuroImage*, *199*, 81–86.

Collins, J.J., De Luca, C.J. (1993). Open-loop and closed-loop control of posture: a random-walk analysis of center-of-pressure trajectories. *Experimental Brain Research*, *95*(2), 308–18.

Crowell, S.E., Butner, J.E., Wiltshire, T.J., Munion, A.K., Yaptangco, M., Beauchaine, T.P. (2017). Evaluating emotional and biological sensitivity to maternal behavior among self-injuring and depressed adolescent girls using nonlinear dynamics. *Clinical Psychological Science*, *5*(2), 272–85.

Cui, X., Bryant, D.M., Reiss, A.L. (2012). NIRS-based hyperscanning reveals increased interpersonal coherence in superior frontal cortex during cooperation. *NeuroImage*, *59*(3), 2430–37.

Dale, R., Fusaroli, R., Duran, N.D., Richardson, D.C. (2013). Chapter two—the self-organization of human interaction. In: Ross, B.H. editor. *Psychology of Learning and Motivation* Waltham, MA, Vol. 59, pp. 43–95. Waltham, MA: Academic Press.

Dalla Porta, L., Matias, F.S., Dos Santos, A.J., et al. (2019). Exploring the phase-locking mechanisms yielding delayed and anticipated synchronization in neuronal circuits. *Frontiers in Systems Neuroscience*, *13*, 1–9

Delaherche, E., Chetouani, M., Mahdhaoui, A., Saint-Georges, C., Viaux, S., Cohen, D. (2012). Interpersonal synchrony: a survey of evaluation methods across disciplines. *IEEE Transactions on Affective Computing*, *3*(3), 349–65.

Dumas, G., Lachat, F., Martinerie, J., Nadel, J., George, N. (2011). From social behaviour to brain synchronization: review and perspectives in hyperscanning. *IRBM*, *32*(1), 48–53.

Dumas, G., Guzman, G.C., De, Tognoli, E., Kelso, J.A.S. (2014). The human dynamic clamp as a paradigm for social interaction. *Proceedings of the National Academy of Sciences*, *111*(35), E3726–E3734.

Engle, R. F., Granger, C. W. J. (1987). Co-Integration and Error Correction: Representation, Estimation, and Testing. *Econometrica*, *55*(2), 251–276 JSTOR.

Fairhurst, M.T., Janata, P., Keller, P.E. (2013). Being and feeling in sync with an adaptive virtual partner: brain mechanisms underlying dynamic cooperativity. *Cerebral Cortex*, *23*(11), 2592–600.

Frank, T.D., Silva, P.L., Turvey, M.T. (2012). Symmetry axiom of Haken–Kelso–Bunz coordination dynamics revisited in the context of cognitive activity. *Journal of Mathematical Psychology*, *56*(3), 149–65.

Fujiwara, K., Kimura, M., Daibo, I. (2019). Rhythmic features of movement synchrony for bonding individuals in dyadic interaction. *Journal of Nonverbal Behavior*, *44*(1), 173–193.

Fusaroli, R., Tylén, K. (2016). Investigating conversational dynamics: interactive alignment, interpersonal synergy, and collective task performance. *Cognitive Science*, *40*(1), 145–71.

Goldberger, A.L., Amaral, L.A.N., Hausdorff, J.M., Ivanov, P.C., Peng, C.-K., Stanley, H.E. (2002). Fractal dynamics in physiology: alterations with disease and aging. *Proceedings of the National Academy of Sciences*, *99*(suppl 1), 2466–72.

Golland, Y., Arzouan, Y., Levit-Binnun, N. (2015). The mere co-presence: synchronization of autonomic signals and emotional responses across co-present individuals not engaged in direct interaction. *PLoS One*, *10*(5), e0125804.

Gorman, J.C. (2014). Team coordination and dynamics: two central issues. *Current Directions in Psychological Science*, *23*(5), 355–60.

Gorman, J.C., Grimm, D.A., Stevens, R.H., Galloway, T., Willemsen-Dunlap, A.M., Halpin, D.J. (2019). Measuring real-time team cognition during team training. *Human Factors: The Journal of the Human Factors and Ergonomics Society*, *62*(5), 825–860.

Gorman, J.C., Martin, M.J., Dunbar, T.A., et al. (2016). Cross-level effects between neurophysiology and communication during team training. *Human Factors*, *58*(1), 181–99.

Gottman, J.M. (2014). *Principia Amoris: the New Science of Love*. New York: Routledge.

Grinsted, A., Moore, J.C., Jevrejeva, S. (2004). Application of the cross wavelet transform and wavelet coherence to geophysical time series. *Nonlinear Processes in Geophysics*, *11*(5/6), 561–66.

Guastello, S.J., Peressini, A.F. (2017). Development of a synchronization coefficient for biosocial interactions in groups and teams. *Small Group Research*, *48*(1), 3–33.

Haken, H., Kelso, J.A.S., Bunz, H. (1985). A theoretical model of phase transitions in human hand movements. *Biological Cybernetics*, *51*(5), 347–56.

Henelius, A.K. (2016). *Colibri*. https://github.com/bwrc/colibri

Hoover, A., Singh, A., Fishel-Brown, S., Muth, E. (2012). Real-time detection of workload changes using heart rate variability. *Biomedical Signal Processing and Control*, *7*(4), 333–41.

Hurtado, J.M., Rubchinsky, L.L., Sigvardt, K.A. (2004). Statistical method for detection of phase-locking episodes in neural oscillations. *Journal of Neurophysiology*, *91*(4), 1883–98.

Issartel, J., Bardainne, T., Gaillot, P., Marin, L. (2015). The relevance of the cross-wavelet transform in the analysis of human interaction—a tutorial. *Frontiers in Psychology*, 5, 1–9

Jha, R., Senroy, N. (2018). Wavelet ridge technique based analysis of power system dynamics using measurement data. *IEEE Transactions on Power Systems*, *33*(4), 4348–59.

Kantz, H., Schreiber, T. (2003). November *Nonlinear Time Series Analysis*. Cambridge, UK: Cambridge Core.

Keller, P.E., Novembre, G., Hove, M.J. (2014). Rhythm in joint action: psychological and neurophysiological mechanisms for real-time interpersonal coordination. *Philosophical Transactions of the Royal Society B: Biological Sciences*, *369*(1658), 20130394.

Kugler, P.N., Turvey, M.T. (1987). *Information, Natural Law, and the Self-assembly of Rhythmic Movement*. Hillsdale, NJ: Lawrence Earlbaum Associates.

Kurz, M.J., Stergiou, N. (2002). Effect of normalization and phase angle calculations on continuous relative phase. *Journal of Biomechanics*, *35*(3), 369–74.

Lai, Y.-C., Frei, M.G., Osorio, I. (2006). Detecting and characterizing phase synchronization in nonstationary dynamical systems. *Physical Review E*, *73*(2), 026214.

Le Van Quyen, M., Foucher, J., Lachaux, J.-P., et al. (2001). Comparison of Hilbert transform and wavelet methods for the analysis of neuronal synchrony. *Journal of Neuroscience Methods*, *111*(2), 83–98.

Likens, A.D., Amazeen, P.G., Stevens, R., Galloway, T., Gorman, J.C. (2014). Neural signatures of team coordination are revealed by multifractal analysis. *Social Neuroscience*, *9*(3), 219–34.

Likens, A.D., Amazeen, P.G., West, S.G., Gibbons, C.T. (2019). Statistical properties of Multiscale Regression Analysis: simulation and application to human postural control. *Physica A: Statistical Mechanics and Its Applications*, *532*, 121580.

Louwerse, M.M., Dale, R., Bard, E.G. Jeuniaux, P. (2012). Behavior matching in multimodal communication is synchronized. *Cognitive Science*, *36*(8), 1404–26.

Mayo, O., Gordon, I (2020). In and out of synchrony–Behavioral and physiological dynamics of dyadic interpersonal coordination.. *Psychophysiology*, *57*(6), e13574, 1–15.

Moulder, R.G., Boker, S.M., Ramseyer, F., Tschacher, W. (2018). Determining synchrony between behavioral time series: an application of surrogate data generation for establishing falsifiable null-hypotheses. *Psychological Methods*, *23*(4), 757–73.

Okazaki, S., Hirotani, M., Koike, T., et al. (2015). Unintentional interpersonal synchronization represented as a reciprocal visuo-postural feedback system: a multivariate autoregressive modeling approach. *PLoS One*, *10*(9), e0137126.

Palumbo, R.V., Marraccini, M.E., Weyandt, L.L., et al. (2017). Interpersonal autonomic physiology: a systematic review of the literature. *Personality and Social Psychology Review*, *21*(2), 99–141.

Perry, N.S., Baucom, K.J.W., Bourne, S., et al. (2017). Graphic methods for interpreting longitudinal dyadic patterns from repeated-measures actor–partner interdependence models. *Journal of Family Psychology*, *31*(5), 592–603.

Podobnik, B., Stanley, H. E. (2008). Detrended cross-correlation analysis: A new method for analyzing two nonstationary time series. *Physical Review Letters*, *100*(8), 084102-1–084102-4.

Quiroga, R.Q., Kraskov, A., Kreuz, T., Grassberger, P. (2002). On the performance of different synchronization measures in real data: a case study on EEG signals. *Physical Review E*, *65*(4), 041903.

Core Team, R.. (2018). *R: A language and Environment for Statistical Computing* (3.5.1) [Computer software].

Ramseyer, F., Tschacher, W. (2016). Movement coordination in psychotherapy: synchrony of hand movements is associated with session outcome. A single-case study. *Nonlinear Dynamics, Psychology, and Life Sciences*, *20*(2), 145–66.

Ramseyer, F., Tschacher, W. (2011). Nonverbal synchrony in psychotherapy: coordinated body movement reflects relationship quality and outcome. *Journal of Consulting and Clinical Psychology*, *79*(3), 284–95.

Ramseyer, F., Tschacher, W. (2014). Nonverbal synchrony of head- and body-movement in psychotherapy: different signals have different associations with outcome. *Frontiers in Psychology*, 5, 1–9.

Randall, A.K., Post, J.H., Reed, R.G., Butler, E.A. (2013). Cooperating with your romantic partner: associations with interpersonal emotion coordination. *Journal of Social and Personal Relationships*, *30*(8), 1072–95.

Richardson, M., Garcia, R.L., Frank, T.D., Gregor, M., Marsh, K.L. (2012). Measuring group synchrony: a cluster-phase method for analyzing multivariate movement time-series. *Frontiers in Physiology*, *3*, 1–10.

Richardson, M.J., Marsh, K.L., Isenhower, R.W., Goodman, J.R., Schmidt, R.C. (2007). Rocking together: dynamics of intentional and unintentional interpersonal coordination. *Human Movement Science*, *26*(6), 867–91.

Rosenblum, M.G., Kurths, J., Pikovsky, A., Schafer, C., Tass, P., Abel, H. (1998). Synchronization in noisy systems and cardiorespiratory interaction. *IEEE Engineering in Medicine and Biology Magazine*, *17*(6), 46–53.

Rössler, O.E. (1976). An equation for continuous chaos. *Physics Letters. A*, *57*(5), 397–8.

Schilbach, L. (2019). Using interaction-based phenotyping to assess the behavioral and neural mechanisms of transdiagnostic social impairments in psychiatry. *European Archives of Psychiatry and Clinical Neuroscience*, *269*(3), 273–4.

Schmidt, R.C., Bienvenu, M., Fitzpatrick, P.A., Amazeen, P.G. (1998). A comparison of intra- and interpersonal interlimb coordination: coordination breakdowns and coupling strength. *Journal of Experimental Psychology. Human Perception and Performance*, *24*(3), 884–900.

Schmidt, R.C., Carello, C., Turvey, M.T. (1990). Phase transitions and critical fluctuations in the visual coordination of rhythmic movements between people. *Journal of Experimental Psychology: Human Perception And*, *16*(2), 227–47.

Schmidt, R.C., O'Brien, B. (1997). Evaluating the dynamics of unintended interpersonal coordination. *Ecological Psychology*, *9*(3), 189–206.

Schoenherr, D., Paulick, J., Worrack, S., et al. (2019). Quantification of nonverbal synchrony using linear time series analysis methods: lack of convergent validity and evidence for facets of synchrony. *Behavior Research Methods*, *51*(1), 361–83.

Schürmann, T. (2004). Bias analysis in entropy estimation. *Journal of Physics A: Mathematical and General*, *37*(27), L295–L301.

Shaffer, F., Ginsberg, J.P. (2017). An overview of heart rate variability metrics and norms. *Frontiers in Public Health*, 5, 1–17.

Shahsavari Baboukani, P., Azemi, G., Boashash, B., Colditz, P., Omidvarnia, A. (2019). A novel multivariate phase synchrony measure: application to multichannel newborn EEG analysis. *Digital Signal Processing*, *84*, 59–68.

Small, M., Yu, D., Harrison, R.G. (2001). Surrogate test for pseudoperiodic time series data. *Physical Review Letters*, *87*(18), 188101.

Soczawa-Stronczyk, A.A., Bocian, M., Wdowicka, H., Malin, J. (2019). Topological assessment of gait synchronisation in overground walking groups. *Human Movement Science*, *66*, 541–53.

Spivey, M.J., Grosjean, M. (2005). Continuous attraction toward phonological competitors. *Proceedings of the National Academy of Sciences*, *102*(29), 10393–1098.

Stepp, N., Turvey, M.T. (2010). On strong anticipation. *Cognitive Systems Research*, *11*(2), 148–64.

Stepp, N., Turvey, M.T. (2015). The muddle of anticipation. *Ecological Psychology*, *27*(2), 103–26.

Strang, A.J., Funke, G.J., Russell, S.M., Dukes, A.W., Middendorf, M.S. (2014). Physio-behavioral coupling in a cooperative team task: contributors and relations. *Journal of Experimental Psychology. Human Perception and Performance*, *40*(1), 145–58.

Tary, J.B., Herrera, R.H., van der Baan, M. (2018). Analysis of time-varying signals using continuous wavelet and synchrosqueezed transforms. *Philosophical Transactions. Series A, Mathematical, Physical, and Engineering Sciences*, *376*, 2126.

Tass, P., Rosenblum, M.G., Weule, J., et al. (1998). Detection of n: M phase locking from noisy data: application to magnetoencephalography. *Physical Review Letters*, *81*(15), 3291–94.

Ting, L.H., Allen, J.L. (2013). Neuromechanics of postural control. In: Jaeger, D., Jung, R. editors. *Encyclopedia of Computational Neuroscience*. Springer, New York, NY: 1–4.

Tognoli, E., Lagarde, J., DeGuzman, G.C., Kelso, J.A.S. (2007). The phi complex as a neuromarker of human social coordination. *Proceedings of the National Academy of Sciences*, *104*(19), 8190–95.

Torrence, C., Campo, G. P. (1998). A Practical Guilde to Wavelet Analysis. *Bulletin of the American Meteorogical Society*, *79*(1), 61–78.

Wallot, S., Leonardi, G. (2018). Analyzing multivariate dynamics using cross-recurrence quantification analysis (crqa), diagonal-cross-recurrence profiles (dcrp), and multidimensional recurrence quantification analysis (mdrqa)'a tutorial in r. Frontiers in psychology, 9(2232), 1–21.

Wang, C., Li, H., Jia, L., Li, F., Wang, J. (2020). Theta band behavioral fluctuations synchronized interpersonally during cooperation. *Psychonomic Bulletin & Review*, 27, 563–570.

Washburn, A., Kallen, R.W., Lamb, M., Stepp, N., Shockley, K., Richardson, M.J. (2019). Feedback delays can enhance anticipatory synchronization in human-machine interaction. *PLoS One*, *14*, 8.

Wiltshire, T.J., Butner, J.E., Fiore, S.M. (2018). Problem-solving phase transitions during team collaboration. *Cognitive Science*, *42*(1), 129–67.

Wiltshire, T.J., Philipsen, J.S., Trasmundi, S.B., Jensen, T.W., Steffensen, S.V. (2020). Interpersonal coordination dynamics in psychotherapy: a systematic review. *Cognitive Therapy and Research*.

Wiltshire, T.J., Steffensen, S.V., Fiore, S.M. (2019). Multiscale movement coordination dynamics in collaborative team problem solving. *Applied Ergonomics*, *79*, 143–151.

Winter, D.A. (2009). *Biomechanics and Motor Control of Human Movement* Wiley. Hoboken, NJ, 4th ed.

Zhang, M., Beetle, C., Kelso, J.A.S., Tognoli, E. (2019). Connecting empirical phenomena and theoretical models of biological coordination across scales. *Journal of the Royal Society Interface*, *16*(157), 1–11.

Zhang, M., Kalies, W.D., Kelso, J.A.S., Tognoli, E. (2020). Topological portraits of multiscale coordination dynamics. *Journal of Neuroscience Methods*, 1-12, 108672.